

# Quantitative benchtop $^{19}\text{F}$ NMR spectroscopy: a robust and economical tool for rapid reaction optimization

G. Heinrich<sup>1</sup>, M. Kondratiuk<sup>1</sup>, L. J. Gooßen<sup>1</sup>, M. P. Wiesenfeldt<sup>1,2</sup>

The instrumental analysis of reaction mixtures is usually the rate-determining step in the optimization of chemical processes. Traditionally, reactions are analyzed by gas chromatography (GC), high-performance liquid chromatography (HPLC), or quantitative nuclear magnetic resonance (qNMR) spectroscopy on high-field spectrometers. However, chromatographic methods require elaborate work-up and calibration protocols, while high-field NMR spectrometers are expensive to purchase and operate. We herein disclose an inexpensive and highly effective analysis method based on low-field benchtop-NMR spectroscopy. Its key feature is the use of fluorine-labeled model substrates which, due to the wide chemical shift range and high sensitivity of  $^{19}\text{F}$ , enables separate, quantitative detection of product and by-product signals even on low-field, permanent magnet spectrometers. An external lock / shim device obviates the need for deuterated solvents, permitting the direct, non-invasive measurement of crude reaction mixtures with minimal work-up. The low field-strength allows a homogeneous excitation over a wide chemical shift range, minimizing systematic integration errors. The addition of the correct amount of the non-shifting relaxation agent  $\text{Fe}(\text{acac})_3$  minimizes relaxation delays at full resolution, reducing the analysis time to 32 seconds per sample. The correct choice of processing parameters is also crucial. A step-by-step guideline is provided, the influence of all parameters is discussed, and potential pitfalls are highlighted. The wide applicability of the analytical protocol for reaction optimization is illustrated by three examples: a Buchwald-Hartwig amination, a Suzuki coupling, and a C–H functionalization reaction.

## Introduction

---

### Product analysis as the bottleneck in reaction discovery and process optimization

The discovery, optimization, and scale-up of chemical transformations involves the testing of numerous reaction parameters such as solvents, catalysts, ligands, and additives to find the best set of conditions (Fig. 1, a)<sup>1</sup>. Yields are typically optimized in cycles during which one parameter is varied while all other parameters are held constant. After quantitative analysis, the best iteration is selected and held constant in the next optimization cycle in which the next parameter is varied. This process can be accelerated by smart screening approaches that speed up the initial discovery<sup>2–6</sup> or assess and improve generality<sup>7,8</sup> or sensitivity<sup>9</sup>. Alternatively, design of experiments (DOE) approaches are employed, in which advanced statistical methods allow multiple parameters to be optimized simultaneously<sup>10–16</sup>. In any case, the time required for sample preparation and analytical measurements is the bottleneck of the entire project. The analysis is usually performed sequentially on the same analytical instrument. Thus, the analysis time, which corresponds to the standstill between two optimization cycles, scales linearly with the number of reactions that need to be analyzed, since the design of the next optimization cycle usually depends on the result of the previous cycle<sup>10,12,14,16</sup>.

Reaction analysis is generally performed in situ by integrating representative signals from all components of a reaction mixture relative to an internal standard using gas chromatography (GC), high performance liquid chromatography (HPLC), or quantitative nuclear magnetic resonance (qNMR) spectroscopy. We compared the main analytical methods for two optimization experiments of a catalytic amination reaction regarding analysis time and accuracy without calibration (Fig. 1, b). Isolation of all products by preparative chromatography is time-consuming but gives accurate yields. In-situ GC chromatography takes about 15 minutes plus 3 minutes for work-up, HPLC analysis takes 18 plus 3 minutes, and  $^1\text{H}$  NMR spectroscopy in deuterated solvents takes about 10 minutes for solvent exchange and 1 minute for analysis. As the model substrates carry fluorine atoms, it is also possible to follow the reaction by in situ  $^{19}\text{F}$  NMR analysis. Without prior calibration, GC and HPLC analysis under- or overestimate the yields and  $^{19}\text{F}$  qNMR spectroscopy with default parameters even gives the wrong relative order of yields leading optimization into the wrong direction. We herein disclose a protocol that allows reaction mixtures to be reliably analyzed within seconds by benchtop  $^{19}\text{F}$  qNMR spectroscopy.

### Reaction optimization by chromatographic methods

While reaction analysis by GC and HPLC remains the state-of-the-art, the long analysis time provides a challenge due to the sequential nature. For instance, GC analysis of 10 reactions requires approximately 3 hours and the analysis of a 96-well plate takes as much as 28 hours. This observation has triggered extensive research into more efficient analysis strategies such as MISER chromatography<sup>17</sup>. Furthermore, both GC and HPLC must be calibrated with pure analytes in order to provide accurate yields, as illustrated in Fig. 1, b. However, pure analytes are often difficult to obtain in the early stages of an optimization campaign. In addition, many reactions contain reactive analytes that degrade the stationary phase. For instance, organometallic reagents, including even boronic acids, rapidly degrade GC or HPLC columns leading to large deviations in the detected yields within a series of only 20

<sup>1</sup>Department of Chemistry and Biochemistry, Ruhr-Universität Bochum, D-44801 Bochum, Germany

<sup>2</sup>Max-Planck-Institut für Kohlenforschung, D-45470 Mülheim an der Ruhr, Germany

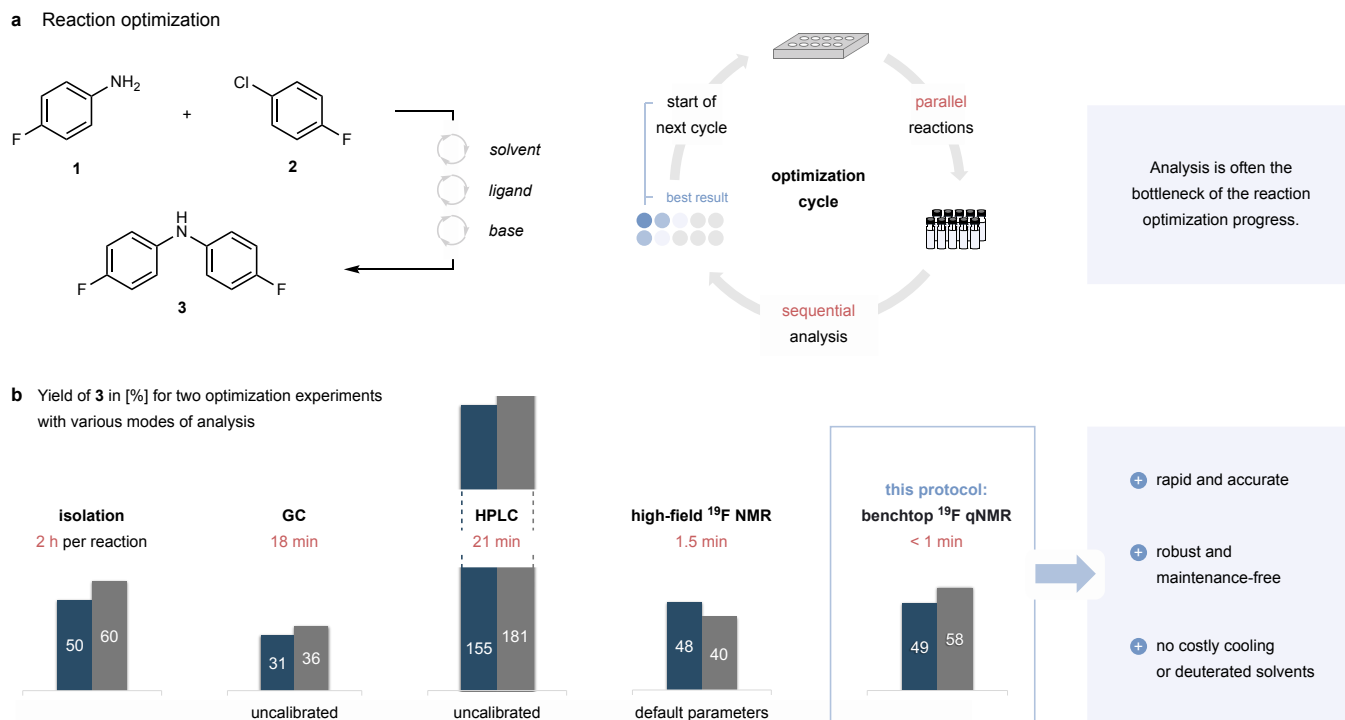


**Fig. 1 | Reaction optimization by benchtop  $^{19}\text{F}$  qNMR spectroscopy.** a) Illustration of a typical reaction optimization cycle for an amination reaction. b) Isolated vs. analytically obtained yields for an amination reaction conducted in DMSO (blue) and toluene (gray) along with the typical analysis time.

samples. Hence, reactive analytes must be removed by a time-consuming work-up prior to analysis. The work-up-procedure tends to remove some of the reaction components, so that the resulting analysis may no longer be representative.

### Reaction optimization by NMR spectroscopy

Reaction analysis by NMR spectroscopy offers several advantages over chromatographic methods<sup>18–20</sup>. First, the analysis can be performed within a short time. Using the default parameters for a  $^1\text{H}$  NMR spectrum, barely 1 minute of measurement time is required. However, additional time is generally needed to exchange the solvent for a deuterated solvent, to avoid dominant solvent signals, and to enable the spectrometer's internal lock and shim. However, this is not necessary when using  $^{19}\text{F}$  NMR spectroscopy in combination with fluorinated tags. Second, no component of the instrument is in direct contact with the analyte, so contamination and damage to the instrument by the sample is not an issue. Third, calibration is not required, since a signal's integral is directly proportional to the number of nuclei in the sample. However, this is only the case after delicate adjustment of the acquisition parameters specifically for quantitative measurement. Most NMR departments provide routine analyses that are optimized for signal resolution rather than realistic integrals. Spectroscopic yields calculated from such spectra can substantially deviate from the true values. Trained experts know how to individually parametrize them for a set of quantitative measurements, but preparative chemists often do not have sufficient knowledge to request measurements with correctly adjusted settings. Furthermore, these adjustments result in long analysis times and high costs per experiment due to expensive liquid helium cooling.

### Advantages of benchtop NMR spectroscopy

In direct comparison with high-field NMR analysis, reaction monitoring by benchtop NMR spectrometers is extremely economical<sup>21–23</sup>. The purchase price of benchtop NMR spectrometers is typically an order of magnitude lower than that of a standard high-field spectrometer and they can be operated and maintained without trained personnel making them accessible for individual research groups in industry and academia. Moreover, such instruments cause almost no operating costs because their permanent magnets do not require helium cooling, and they are usually equipped with an external lock and shim device, obviating the need for expensive deuterated solvents. In contrast to chromatographic instruments, they require much less maintenance since they never come into direct contact with the chemical components of the reaction mixture. We have developed an open-source 3D-printed autosampler for such instruments enabling rapid insertion of samples<sup>24</sup> and increasingly shifted in situ reaction analysis from the GC- and HPLC-based-techniques towards quantitative  $^{19}\text{F}$  qNMR spectroscopy using benchtop NMR spectrometers<sup>24–31</sup>. Herein, we explain how accurate yields can rapidly and reliably be determined using one of the most inexpensive and lowest-field (40.89 MHz) NMR spectrometers on the market. Using an easy-to-follow protocol, reliable quantification of reaction mixtures is achieved on similar instruments, within only 32 seconds, translating to a total analysis time of less than 1 minute per sample including sample preparation.

# Development of the protocol

## Selection of the nucleus

The main challenge in using benchtop spectrometers for reaction optimization is their low field strength, which makes it difficult to meet the requirements for qNMR spectroscopy<sup>18,32,33</sup>: signal selectivity must be high enough to ensure baseline-separation of all relevant signals of analytes and standard, resolution (signal-to-noise ratio (SNR), number of data points) must be sufficient to enable precise integration, and complete relaxation of all nuclei between the scans is required to enable accurate integration. Additionally, the solubility, chemical stability, and inertness of all analytes must be ensured during the time of the measurement. In comparison to high-field instruments, the lower magnetic field of bench-top instruments results in a lower signal selectivity, SNR, and resolution. Reaction monitoring based on <sup>1</sup>H NMR spectroscopy is only possible for simple reaction mixtures due to signal overlap. <sup>19</sup>F NMR spectroscopy is ideal for use with low-field instruments, as <sup>19</sup>F has a wide chemical shift range (>350 ppm) and is highly sensitive due to its 100% natural abundance and high gyromagnetic ratio (40 MHz/T)<sup>34,35</sup>. Like the commonly used <sup>1</sup>H nucleus, <sup>19</sup>F has a nuclear spin of ½, giving first-order spectra. Due to the proverbial stability of C–F bonds<sup>36</sup>, fluorinated groups are mostly chemically innocent, which makes them ideal as spectroscopic labels. Fluorine substituents are of critical importance in medicinal chemistry<sup>37,38</sup>, which has triggered the development of fluorination<sup>39–45</sup> and trifluoromethylation<sup>46–52</sup> methods, so that even elaborate fluorinated motifs are widely available in great structural variety<sup>53–56</sup>. As a result, fluorinated model substrates are available for almost every reaction type.

Indeed, for most reactions that we have investigated in recent years, suitable sets of fluorinated test substrates could be identified for which all reaction components, including minor side products, give baseline-separated, individually detectable signals on our 41 MHz benchtop spectrometers. In the analysis of reaction mixtures, a realistic concentration of the major species after standard reaction work-up is 0.1 M. At this concentration, a more than sufficient SNR of >800 was determined for <sup>19</sup>F nuclei after 16 scans, which is well-above the commonly cited threshold of 150<sup>19,33</sup>. Control experiments confirmed that within 16 scans, the cumulative error of the integrals falls below 3% after suitable signal processing (see SI for details)<sup>57</sup>. This is in the same range as in-situ GC-spectroscopy. Notably, although decoupling methods afford better separated singlets for all reaction components, they must be avoided since the nuclear Overhauser effect (NOE) leads to individual deviations in the integrals<sup>18</sup>.

## The crucial influence of the excitation profile on the integrals

The key challenge when using <sup>19</sup>F NMR to quantify reaction products is to ensure a homogeneous excitation of all nuclei over a wide chemical shift range. Large systematic errors are encountered on high-field instruments, since the signal intensity decreases dramatically with their distance from the center frequency (Fig. 2)<sup>58,59</sup>. Reduced excitation translates to a reduced integral for a reaction component. This effect can be dramatic and is greatly underestimated. When analyzing a 2:1 mixture of trifluoroacetophenone (**4**,  $\delta = -71$  ppm) and hexafluorobenzene (**5**,  $\delta = -163$  ppm) on a 400 MHz high-field spectrometer, the integral of **5** is reduced to only 20% of its expected value when the center frequency of a 90° pulse is set to  $-71$  ppm, at optimal settings for all other parameters (Fig. 2, entries 1 and 2). The excitation profile can be flattened by decreasing the pulse width (entry 3), but this also reduces the signal intensity and thereby the SNR, which must be compensated for by increasing the number of scans (entry 4). At a pulse width of 2  $\mu$ s, which we recommend for analysis on high-field spectrometers, the integral of **5** is still reduced by 4% from its expected value. More accurate quantification of multiple signals with large deviations in the chemical shifts on high-field instruments requires elaborate pulse sequences or overlaying techniques<sup>58,60</sup>. This easily increases the analysis time per sample to over 10 minutes. Quantification of reaction components based on their high-field <sup>19</sup>F NMR signals is only reliable if the signals of all analytes and the internal standard are all almost equidistant from the center frequency.

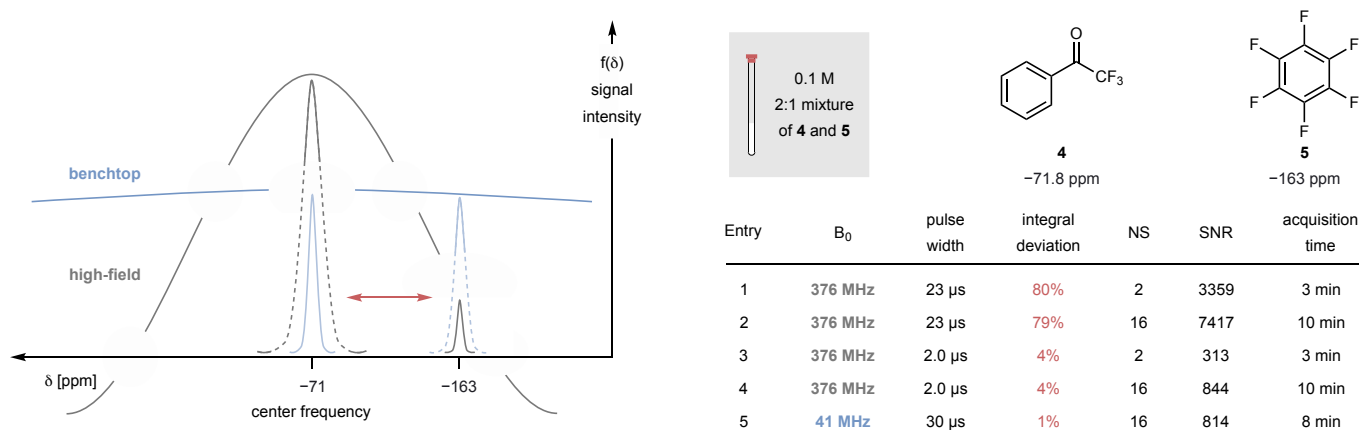


**Fig. 2 | Influence of the excitation profile on integral ratios.** Signal intensity and thus the integral decrease with the distance from the center frequency. The dramatic effect of the profile on the integrals on a high-field spectrometer was demonstrated for a 2:1 mixture of trifluoroacetophenone (**4**) and hexafluorobenzene (**5**). Only a minimal integral deviation was found on the benchtop spectrometer. The deviation on the high-field spectrometer can be minimized by decreasing the pulse width, which also results in a lower SNR. The excitation profiles of high-field and benchtop NMR spectrometers were simulated using an online tool<sup>61</sup>. B<sub>0</sub>, spectrometer frequency. NS, number of scans. SNR, signal-to-noise ratio.

In sharp contrast, the excitation profile of benchtop spectrometers is homogeneous over a wide range due to their low field strengths. The signal of **5** is reduced by less than 1%, even when the center frequency is as far as 92 ppm away from the analyte signal. Thus, if the center frequency is set to the default value of  $-71$  ppm, which is in the middle of the chemical shift range of  $^{19}\text{F}$  nuclei, the effect of the excitation profile on the integration can be neglected.

### The crucial influence of the relaxation delay on the integrals

The main obstacle precluding a rapid analysis protocol based on  $^{19}\text{F}$  NMR spectroscopy is the long measurement time required for the correct integration of all signals. Due to the slow relaxation of some  $^{19}\text{F}$  NMR signals, the dominant component of the measurement time is the relaxation delay. This usually accounts for approximately 95% of the total measurement time (Fig. 3, a). Default settings for  $^{19}\text{F}$  NMR spectroscopy on high-field spectrometers generally use a much too short relaxation delay to reduce the measurement time. Such truncated delays lead to a systematic error, which is often believed to be identical for all analyzed samples so that it might still allow a qualitative comparison of screening experiments. However, we have often experienced that it also causes individual deviations for each sample, which cannot be corrected by calibration measurements. Although the relaxation time is mostly a compound-specific property, it is also subject to external factors such as solvent, pH value, salt concentration<sup>62,63</sup> and the strength of the applied magnetic field<sup>64,65</sup>. Therefore, if the time between scans does not permit complete relaxation of all signals, the reaction environment will affect the integrals unpredictably, misrepresenting the actual yields (Fig. 1, b). Errors caused by overly short measuring times have repeatedly led reaction optimizations into a wrong direction.

The required length of the relaxation delay depends on the spin-lattice relaxation time  $T_1$  of the nucleus in its environment. To ensure 99.9% relaxation of all spins, the repetition time, including both relaxation delay and acquisition time, must be equal to at least 7 times the longest  $T_1$  in the sample<sup>33</sup>. Shorter relaxation delays between two scans will result in residual magnetization along the y-axis ( $M_y$ ), thus falsifying the integration results (Fig. 3, b).

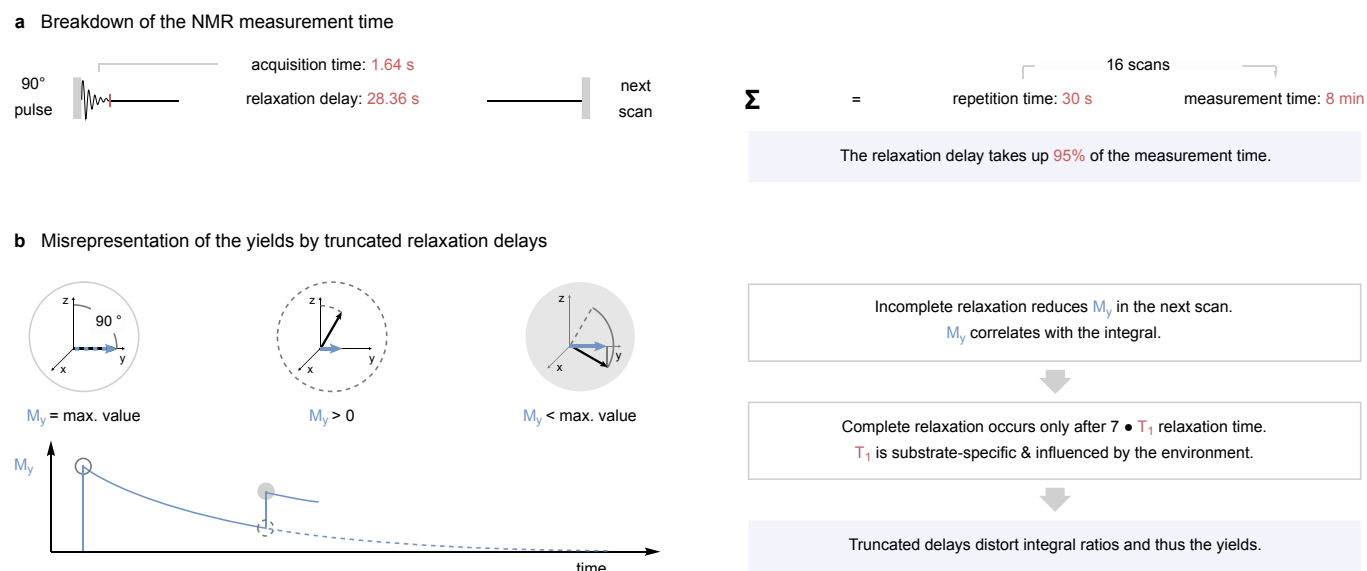
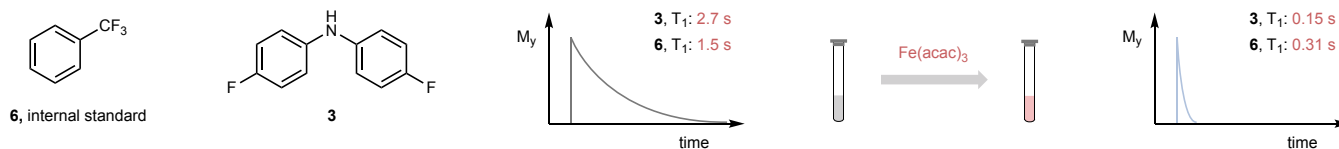


**Fig. 3 | Acquisition time and relaxation delay.** **a**, The relaxation delay is the major component of the measurement time. **b**, Insufficient relaxation delays reduce the integrals, as incomplete relaxation of the magnetic moment along the y-axis ( $M_y$ ) leads to a reduced  $M_y$  for the next scan<sup>66</sup>. This effect results in higher integrals for compounds with low  $T_1$  values precluding relative quantification of reaction components.

### Minimizing analysis times by paramagnetic relaxation agents

Paramagnetic relaxation agents such as  $\text{Cr}(\text{acac})_3$  and the more environmentally benign  $\text{Fe}(\text{acac})_3$  are known to shorten the  $T_1$  relaxation time without changing the chemical shift<sup>67,68</sup>. They have been used, for example, in the accelerated analysis of fluorinated compounds in food and environmental water sources<sup>62,69</sup>. However, most preparative chemists hesitate to use them because they cause line-broadening. We have found that when employing the right agent at the right concentration, the relaxation time can be reduced by a factor of 10 without adversely affecting the spectral resolution (Fig. 4, b, entries 2–4). Our experiments revealed that a concentration of only 6 mmol/L  $\text{Fe}(\text{acac})_3$  (approximately 1 mg per 0.5 mL NMR sample) is ideal for the analysis of screening experiments (entry 4). This concentration has reduced the longest relaxation time in a reaction mixture of benzotrifluoride (**6**) and diarylamine **3** from 2.7 s to 0.31 s (Fig. 4, a) and has reliably reduced the  $T_1$  of all tested  $^{19}\text{F}$ -labelled model substances below 0.5 seconds while maintaining an adequate line width of all signals (see SI for details). Within 16 scans, the SNR is raised well above 150, allowing precise integration. As a result, the required analysis times per sample is dramatically reduced from several minutes to 32 seconds without compromising the quality of the integration.

### a Effect of relaxation agents on the $T_1$ relaxation time



### b Effect of $\text{Fe}(\text{acac})_3$ on the accuracy, line width, precision, and measurement time

Entry	center frequency	$\text{Fe}(\text{acac})_3$ c [mmol/L]	spectrum	integral [%] (actual: 45%)	line width [Hz]	SNR	measurement time
1	-71 ppm	0		44%	2.7	208	8 min
2	-71 ppm	90		50%	15.9	59	32 s
3	-71 ppm	17		45%	5.1	216	32 s
4	-71 ppm	6		46%	3.6	271	32 s
5	-93 ppm	17		47%	4.2	236	32 s

**Fig. 4 | Minimizing analysis time by non-shifting relaxation agents.** **a**, Relaxation agents reduce the  $T_1$  relaxation times allowing a reduction of the repetition time. **b**, Relaxation agents, when used in small amounts, can reduce the measurement time from 8 minutes to 32 seconds. Acquisition parameters:  $B_0 = 41$  MHz, pulse angle:  $90^\circ$ , acquisition time: 1.64 s, NS: 16, relaxation delay: 28.4 or 0.4 s. Post-processing parameters: exponential apodization with 1 Hz LB, 4 times zero-filling, manual phase correction and baseline correction by FID reconstruction (ACD/Labs). Line width and SNR were determined for benzotrifluoride using MNova. NS, number of scans; acac, acetylacetonate; SNR, signal-to-noise ratio; LB, line broadening.

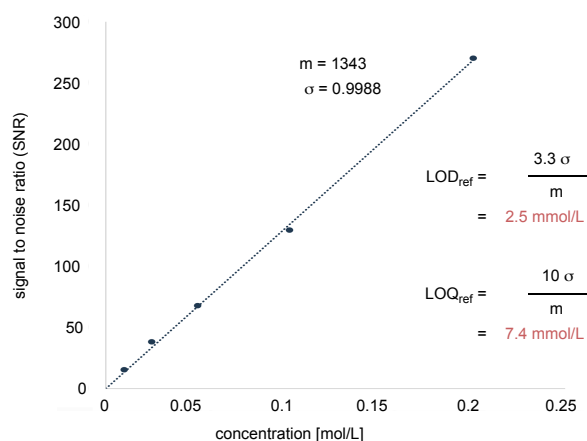
### Limit of detection and limit of quantification

The limit of detection (LOD) and limit of quantification (LOQ) after 16 scans can be determined by plotting the SNR (calculated from the spectra using an MNova software tool)<sup>70</sup> against the analyte concentration (Fig. 5, a). Using the slope ( $m$ ) and the standard deviation ( $\sigma$ ), a limit of detection of 2.5 mmol/L and a limit of quantification of 7.4 mmol/L were determined for **3** (see SI for details)<sup>71</sup>. Thus, when analyzing a reaction mixture that has been diluted to 0.1 mol/L maximum concentration of the limiting reagent, components above 2.5% relative yield can be detected and a reliable integration is possible above 7.4%. These values were determined for a pseudo quintet and are higher for sharp singlets. LOD and LOQ increase with the square root of the number of scans using extended measurement times. This level of precision is sufficient for the intended application.

### Optimal acquisition and post-processing parameters

Control experiments showed that the acquisition time has little effect on the integration, so that standard values can be used. Values between 1.6 s and 3.2 s neither led to FID truncation nor to recording of excessive noise (see SI for details). For the benchtop-NMR spectrometer, slight deviations in the distance of signals from the center frequency do not lead to detectable differences in the integrals. For example, shifting the center frequency from its default value of -71 ppm to the equidistant value of -93 ppm does not result in a difference in the integrals of the signals at -63 and -123 ppm (Fig. 4, b, entry 5).

Proper post-processing of the obtained data is critical to optimize the SNR and allow reliable integration without eliminating signals of trace side products from the spectrum (see SI for details). The use of an exponential apodization function (EM) is highly beneficial as it emphasizes the early parts of the FID signal, thus improving the signal intensity at the expense of the line width. The extent of apodization is given by the line broadening (LB) factor. An LB of 1–2 Hz was optimal for us on a benchtop spectrometer (Fig. 5, b, entries 1 and 2), while 0.2 Hz is sufficient on a high-field spectrometer. The digital resolution is further improved by applying zero filling to the FID, which increases the number of data points. A factor of 2–4 is optimal (entry 3). After Fourier transformation (FT) of the FID, phase- and baseline correction must be performed (entries 4 and 5). Automatic phase correction by the NMR software using default parameters is usually sufficient. Polynomial fits or FID reconstruction typically give good results for the baseline correction. Powerful baseline correction methods such as the Whittaker smoother should only be applied with caution, since these tend to smooth out small signals, suggesting the absence of minor side products. Finally, the internal standard can also be used as chemical shift reference. Referencing all spectra to the shift of the internal standard simplifies the selection of the integral regions.

**a** Determination of the limit of detection**b** Influence of post-processing on the spectrum

Entry	post-processing	spectrum	line width [Hz]	SNR	integral [%] (actual: 45%)
1	none		2.7	45	49%
2	apodization		3.7	131	50%
3	+ 0-filling		3.6	128	48%
4	+ phase correction		3.6	268	47%
5	+ baseline correction		3.6	271	46%

**Fig. 5 | Optimal post-processing parameters and limit of detection.** **a**, The limit of detection of this protocol at 16 scans was determined to be 2.5 mmol/L for a pseudo quintet while the limit of quantification was 7.4 mmol/L. **b**, Correct post-processing is critical to ensure accuracy and precision. Acquisition parameters:  $B_0 = 41$  MHz, pulse angle:  $90^\circ$ , acquisition time: 1.64 s, NS: 16, repetition time: 2.0 s. Post-processing parameters: exponential apodization with 1 Hz LB, 4 times zero-filling, manual phase correction and baseline correction by FID reconstruction (ACD/Labs). Line width and SNR were determined by MNova for benzotrifluoride. NS, number of scans; acac, acetylacetonate; SNR, signal-to-noise ratio; LB, line broadening; LOD, limit of detection; LOQ, limit of quantification.

As illustrated by the three application cases, the main component of reaction mixtures can be reliably quantified within 32 seconds when using the following parameters:

**Optimal acquisition parameters:**

Field strength:  $B_0 = 40.89$  MHz, Pulse angle:  $90^\circ$ , Sample concentration: 0.1 M, acquisition time: 1.64 s, number of scans: 16. Repetition time:  $\geq 7 \times T_1$ .

**Optimal post processing parameters:**

Exponential apodization: 1–2 Hz of LB, zero filling: 2–4x, phasing and baseline correction: on an individual basis.

## Applications

We have applied this protocol to the optimization of a Buchwald-Hartwig amination reaction, a Suzuki cross-coupling reaction, and a C–H arylation reaction. The general workflow for reaction optimization is exemplified below for the example of a Buchwald-Hartwig amination.

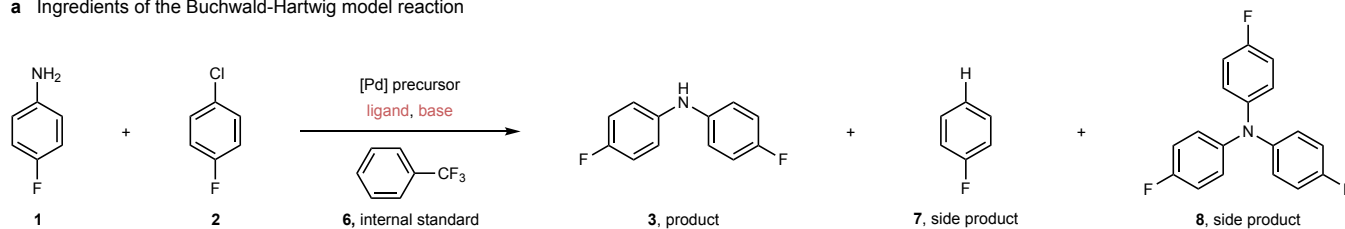
For the Buchwald-Hartwig amination<sup>72,73</sup>, our research question was how Y-Phos ligands<sup>29</sup> would compare with established ligands with regard to activity and selectivity. The workflow starts with the identification of a suitable test reaction. The reaction of *p*-chloroanisole with aniline would have been a typical model reaction for analysis by GC, since this substrate combination allows all substrates, products, and side products to be detected. A rather similar substrate combination, namely the coupling of *p*-chlorofluorobenzene (**2**) with *p*-fluoroaniline (**1**, Fig. 6, a), is a good first choice for analysis by  $^{19}\text{F}$  NMR. The coupling affects the electronic properties of the carbon atoms bearing the nitrogen and chlorine atoms in the substrates and due to the conjugation with the aromatic ring also that of the fluorine substituent in *para*-position thus rendering signal separation of the  $^{19}\text{F}$  NMR spectrum of the product mixture likely. Besides the substrates **1** and **2**, and the diaryl amine product **3**, one would expect to see fluorobenzene (**7**) as a side product under non-optimal conditions, resulting from competing dehalogenation. The  $^{19}\text{F}$  NMR spectrum of a typical reaction mixture obtained under non-optimal conditions shows clearly separated signals for all substrates, products, and side products (Fig. 6, b). If the signals of the reaction components are too close to each other, another of the many possible model reactions could have been chosen, for example with *o*-chlorofluorobenzene as the aryl nucleophile. The next step is to choose an internal standard that is inert under the reaction conditions, does not overlap with any of these compounds, and has similar solubility properties. These prerequisites are fulfilled for benzotrifluoride (**6**).

Using an authentic or a manually prepared reaction mixture consisting of internal standard, products, and side products, the  $T_1$  values of all components can be determined in a single experiment. Without a non-shifting relaxation reagent, the longest  $T_1$ , which is recorded for *p*-chlorofluorobenzene, is 3.0 seconds. In the presence of 6 mmol/L of  $\text{Fe}(\text{acac})_3$ , all  $T_1$  values are shortened to 0.15–0.31 seconds while the effect on the spectral resolution is barely detectable. This control experiment ensures that 2 second scans are long enough to allow full relaxation of all spins.

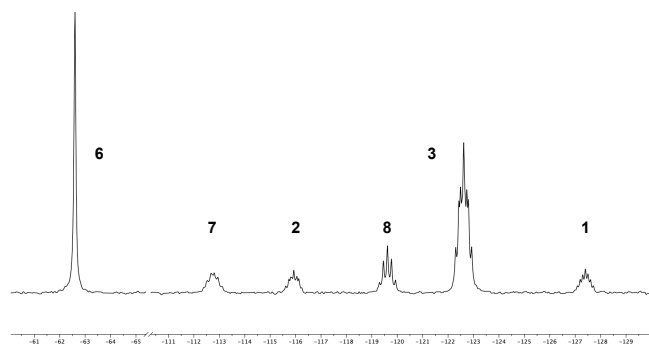
In order to minimize the influence of the reaction solvent and additives on the chemical shift and relaxation of the reaction components, the screening experiments were diluted with 0.3–0.6 mL of a 2.5 M  $\text{Fe}(\text{acac})_3$  solution in toluene and filtered into the NMR tubes. These were subjected to  $^{19}\text{F}$  analysis using the standard parameters described above, resulting in a total analysis time of 32 seconds

per sample. Repeated measurements of representative samples confirmed that the cumulative error caused by work-up and analysis is less than 3–5% of the absolute values, which is almost identical to that observed with GC analysis. Tables 1 and 2 in the chapter “anticipated results” show that the spectroscopic yields obtained within 32 seconds show only minimal deviations from those obtained using conventional methods.

**a** Ingredients of the Buchwald-Hartwig model reaction



**b**  $^{19}\text{F}$  NMR spectrum of the model reaction mixture



**c**  $T_1$  relaxation times in toluene

1	2	3	4	7	8
3.0 s	3.0 s	2.7 s	1.5 s	2.9 s	1.9 s
↓ $\text{Fe}(\text{acac})_3$					
1	2	3	4	7	8
0.25 s	0.25 s	0.15 s	0.31 s	0.29 s	0.22 s

**Fig. 6 | Application of the protocol to a Buchwald-Hartwig amination reaction. a**, Model reaction and substrates, including anticipated side products. **b**,  $^{19}\text{F}$  NMR spectrum of the model reaction mixture in toluene showing baseline-separation of all signals. **c**,  $T_1$  relaxation times of the model substrates in toluene with and without addition of 2 mg/mL (6 mmol/L)  $\text{Fe}(\text{acac})_3$ . The longest  $T_1$  time is reduced from 3.0 s to 0.31 s.

Likewise, the protocol was applied to the optimization of a Suzuki coupling in a “green” solvent using sterically hindered *ortho*-trifluoromethyl-phenylboronic acid (**9**) and *p*-chlorofluorobenzene (**2**) as model substrates (Fig. S8). Optimization of the C–H arylation reaction proceeded using 2-fluorobenzoic acid (**12**) and 1-chloro-4-trifluoromethylbenzene (**13**, Fig. S9)<sup>74</sup>. In this case, post-modification by quantitative methylation was key to ensure signal separation for all relevant species. In both cases, addition of  $\text{Fe}(\text{acac})_3$  enabled reliable quantification of all reaction components within 32 s analysis time (Tables 3–5). See SI for further details.

## Results

The yields of the optimization experiments for the Buchwald-Hartwig amination, the Suzuki cross-coupling, and the C–H arylation reactions were determined using the described procedures via equation 1 (see SI for details). The results obtained using our protocol for rapid measurements were benchmarked against the values obtained using state-of-the-art measurement parameters with elongated repetition times in the absence of a relaxation agent. In all cases, both results were within error of one-another.

$$\text{Yield [\%]} = \frac{I_{\text{analyte}}}{N_{\text{analyte}}} * EQ_{\text{standard}} * 100 \quad (1)$$

$I_{\text{analyte}}$  = integral of the analyte signal,  $N_{\text{analyte}}$  = number of nuclei of the analyte signal,  $EQ_{\text{standard}}$  = equivalents of the internal standard.

### Results for the Buchwald-Hartwig amination

Table 1 compares the relative content of starting materials, products and side products obtained with our 32 second qNMR protocol with those obtained with a state-of-the-art  $^{19}\text{F}$  quantitative NMR measurement. All data points are within a 2% error range.

**Table 1** | Ligand screening of the Buchwald-Hartwig amination.

entry	ligand	amount of 1 [%]		amount of 2 [%]		amount of 3 [%]		amount of 7 [%]		amount of 8 [%]	
		repetition time		repetition time		repetition time		repetition time		repetition time	
		30 s	2 s + Fe	30 s	2 s + Fe	30 s	2 s + Fe	30 s	2 s + Fe	30 s	2 s + Fe
1	BrettPhos	14	12	0	0	98	100	0	0	0	0
2	<i>t</i> BuJohnPhos	108	108	100	101	0	0	0	1	0	0
3	DavePhos	96	92	88	85	11	8	1	0	0	0
4	SPhos	78	79	67	69	32	31	0	0	3	0
5	RuPhos	49	47	36	34	63	61	0	1	0	0
6	<i>t</i> BuXPhos	106	107	96	97	1	1	0	0	0	0
7	XPhos	14	11	0	0	97	99	0	0	0	0

**Acquisition parameters:** internal standard: benzotrifluoride,  $B_0 = 40.89$  MHz, pulse angle:  $90^\circ$ , number of scans: 16, acquisition time: 1.64 s, repetition time as indicated. 2 mg/mL (6 mmol/L) of  $\text{Fe}(\text{acac})_3$  was used as relaxation agent for 2 s of repetition time.

BrettPhos (Table 1, entry 1) and XPhos (entry 7) both gave near-quantitative yields of the desired product **3** with complete conversion of the aryl chloride **2**. The amounts of protodehalogenated side product **7** and triarylamine side product **8** were below the limit of detection.

**Table 2** | Base screening of the Buchwald-Hartwig amination.

entry	base	amount of 1 [%]		amount of 2 [%]		amount of 3 [%]		amount of 7 [%]		amount of 8 [%]	
		repetition time		repetition time		repetition time		repetition time		repetition time	
		30 s	2 s + Fe	30 s	2 s + Fe	30 s	2 s + Fe	30 s	2 s + Fe	30 s	2 s + Fe
1	KOtBu	13	14	0	1	96	100	0	0	0	0
2	NaOtBu	24	21	7	8	93	94	0	0	0	0
3	$\text{K}_2\text{CO}_3$	118	119	100	101	1	1	0	1	0	0
4	CsF	118	118	100	100	1	1	1	0	0	0
5	LiHMDS	22	21	1	1	60	61	1	0	17	16
6	NaHMDS	16	16	1	1	102	102	0	0	0	0
7	<i>n</i> BuLi	47	50	30	31	44	45	1	0	5	5

**Acquisition parameters:** internal standard: benzotrifluoride,  $B_0 = 40.89$  MHz, pulse angle:  $90^\circ$ , number of scans: 16, acquisition time: 1.64 s, repetition time as indicated. 2 mg/mL (6 mmol/L) of  $\text{Fe}(\text{acac})_3$  was used as relaxation agent for 2 s of repetition time.

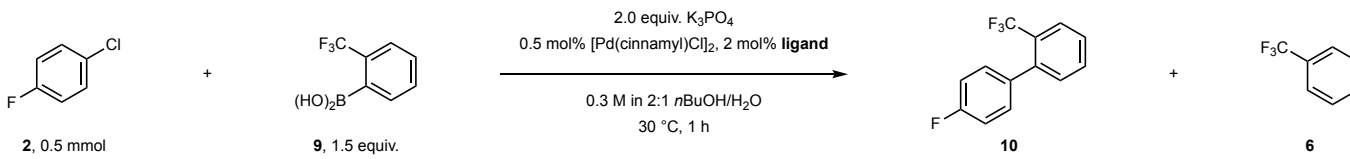
The base screening (Table 2) indicated that alkoxide bases like KOtBu or amide bases like NaHMDS are ideal (Table 2, entries 1, 2, and 6). Lithium bases caused the formation of side products and resulted in measurable deviations of the sum of all fluorinated species from the value expected based on the stoichiometry (entries 5 and 7). We attribute this observation to a defluorination side reaction.



## Results for the Suzuki reaction

In table 3, the product analysis with our 32-second-long qNMR protocol is compared with that obtained with a state-of-the-art  $^{19}\text{F}$  quantitative NMR measurement.

**Table 3** | Ligand screening of the Suzuki reaction.



entry	ligand	amount of <b>2</b> [%]		amount of <b>9</b> [%]		amount of <b>10-F</b> [%]		amount of <b>10-CF<sub>3</sub></b> [%]		amount of <b>6</b> [%]	
		repetition time		repetition time		repetition time		repetition time		repetition time	
		30 s	2 s + Fe	30 s	2 s + Fe	30 s	2 s + Fe	30 s	2 s + Fe	30 s	2 s + Fe
1	XPhos	1	2	4	7	102	97	102	98	36	38
2	tBuXPhos	29	26	1	1	66	65	66	65	85	83
3	DavePhos	59	59 (59 <sup>a</sup> )	2	2 (2 <sup>a</sup> )	27	31 (31 <sup>a</sup> )	32	32 (32 <sup>a</sup> )	119	104 (122 <sup>a</sup> )
4	RuPhos	32	36	3	2	64	65	61	62	69	70
5	SPhos	74	74	1	1	21	22	22	20	131	126

**Acquisition parameters:** internal standard: 1,4-difluorobenzene,  $B_0 = 40.89$  MHz, pulse angle:  $90^\circ$ , number of scans: 16, acquisition time: 1.64 s, repetition time as indicated. 2 mg/mL (6 mmol/L) of  $\text{Fe}(\text{acac})_3$  was used as relaxation agent for 2 s of repetition time. <sup>a</sup>yield was measured with 3 s repetition time.

While the yields obtained with the two methods were mostly within the expected error margin of 2%, the yield of the protodeborylated side product **6** deviated by as much as 15% from that obtained in the control measurement (Table 3, entry 3). This outlier was traced back to the influence of an orthoboric acid side product. The presence of this Lewis-acidic compound almost doubled the  $T_1$  values of the reaction components (Fig. 9). Thus, full relaxation no longer occurred within the 2 seconds of repetition time. However, correct integrals were obtained when increasing the repetition time to 3 s (measurement time: 48 s). This is a rare case, in which we had to re-adjust the repetition time of a protocol that had been validated for the initial reaction conditions. It shows that it can be beneficial to add an extra 50% to the initially measured longest  $T_1$  value when calculating the minimal repetition time.

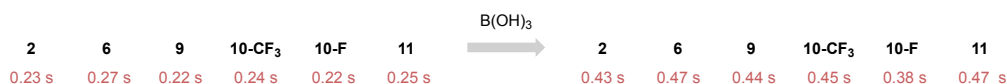
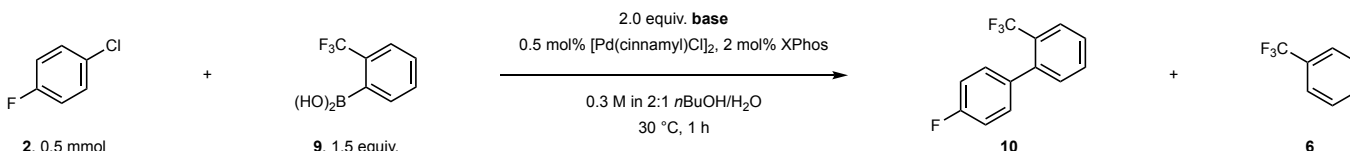


**Fig. 6** | Effect of  $\text{B}(\text{OH})_3$  on the  $T_1$  relaxation times of the model mixture of the Suzuki reaction.

Following selection of XPhos as ligand, we conducted a base screening (Table 4). Based on these results,  $\text{K}_3\text{PO}_4$  was quickly identified as the optimal base (Table 4, entry 1). Under these basic conditions, the repetition time of 2 seconds was sufficient.

**Table 4** | Base screening of the Suzuki reaction.



entry	base	amount of <b>2</b> [%]		amount of <b>9</b> [%]		amount of <b>10-F</b> [%]		amount of <b>10-CF<sub>3</sub></b> [%]		amount of <b>6</b> [%]	
		repetition time		repetition time		repetition time		repetition time		repetition time	
		30 s	2 s + Fe	30 s	2 s + Fe	30 s	2 s + Fe	30 s	2 s + Fe	30 s	2 s + Fe
1	$\text{K}_3\text{PO}_4$	3	1	45	46	100	96	102	97	3	3
2	KOH	1	2	6	5	99	95	100	94	72	66
3	KOtBu	3	3	4	3	94	90	96	91	59	56
4	$\text{K}_2\text{CO}_3$	80	77	3	2	12	8	14	14	11	9
5	KOAc	89	86	1	1	2	3	2	2	85	88

**Acquisition parameters:** internal standard: 1,4-difluorobenzene,  $B_0 = 40.89$  MHz, pulse angle:  $90^\circ$ , number of scans: 16, acquisition time: 1.64 s, repetition time as indicated. 2 mg/mL (6 mmol/L) of  $\text{Fe}(\text{acac})_3$  was used as relaxation agent for 2 s of repetition time.

## Results for the C–H arylation

Table 5 compares the results of the 32-second long rapid analysis and the state-of-the-art qNMR analysis of reaction mixtures obtained when optimizing the conditions of a catalytic C–H activation. In this example, the influence of the ruthenium-precursor on the catalytic arylation of benzoic acids with aryl chlorides is evaluated<sup>74</sup>.

**Table 5 |** Precursor screening for the C–H activation.

1.1 equiv.  $\text{K}_2\text{CO}_3$ , 4 mol% or 8 mol%  
**precursor** 4 mol% or 8 mol% *D,L*-pipecolinic acid  
 0.17 M in NMP, 120 °C, 18 h  
 then 2.5 equiv. MeI, 3.0 equiv.  $\text{K}_2\text{CO}_3$   
 0.1 M in NMP, 60 °C, 2 h

entry	ligand	amount of <b>12Me</b> [%]		amount of product <b>14Me</b> [%]		amount of <b>15Me</b> [%]	
		repetition time		repetition time		repetition time	
		30 s	2 s + Fe	30 s	2 s + Fe	30 s	2 s + Fe
1	$[\text{Ru}(\rho\text{-cym})\text{Cl}_2]_2$ 4 mol%	36	33	56	51	0	0
2	$[\text{Ru}(\text{PPh}_3)_3\text{Cl}_2]$ 4 mol%	101	103	0	0	0	0
3	$[\text{Ru}(\text{PPh}_3)_3\text{Cl}_2]$ 8 mol%	98	100	0	0	0	0
4	$[\text{Ru}(\text{COD}(2\text{-Me-allyl})_2)]_2$ 4 mol%	99	100	1	0	0	0
5	$[\text{Ru}(\text{COD}(2\text{-Me-allyl})_2)]_2$ 8 mol%	96	93	4	3	0	0
6	$[\text{Ru}(\text{acac})_3]$ 4 mol%	71	74	26	21	0	0
7	$[\text{Ru}(\text{acac})_3]$ 8 mol%	102	102	0	0	0	0
8	$[\text{RuCl}_3] \times \text{H}_2\text{O}$ 4 mol%	95	94	5	4	0	0
9	$[\text{RuCl}_3] \times \text{H}_2\text{O}$ 8 mol%	100	103	0	2	0	0
10	$[\text{Ru}(\text{PhH})\text{Cl}_2]_2$ 4 mol%	47	46	45	43	0	0
11 <sup>a</sup>	$[\text{Ru}(\rho\text{-cym})\text{Cl}_2]_2$ 4 mol%	6	6	89 <sup>b</sup>	87 <sup>b</sup>	0	0

**Acquisition parameters:** internal standard: 1,4-difluorobenzene,  $B_0 = 40.89$  MHz, pulse angle:  $90^\circ$ , number of scans: 16, acquisition time: 1.64 s, repetition time as indicated. 2 mg/mL (6 mmol/L) of  $\text{Fe}(\text{acac})_3$  was used as relaxation agent for 2 s of repetition time. <sup>a</sup>Chlorobenzene was used as a coupling partner instead of **13**. <sup>b</sup>Methyl 3-fluoro-[1,1'-biphenyl]-2-carboxylate is obtained as product instead of **14**.

All values are within the expected error margin of 3%.  $[\text{Ru}(\rho\text{-cym})\text{Cl}_2]_2$  and  $[\text{Ru}(\text{PhH})\text{Cl}_2]_2$  were identified as the best precursors in this exemplary screen (Table 5, entries 1 and 10). All yields are relatively low, which is due to the low reactivity of the model substrate. A control experiment conducted with non-fluorinated aryl chloride gave the same results as reported in literature<sup>74</sup>.

## Limitations

The presented protocol allows accurate and general quantification of mixtures of fluorinated compounds. However, there are some limitations. Naturally, only fluorinated compounds can be measured. This requires the introduction of a fluorinated probe. While fluorine is chosen in part for its relative inertness, the optimal reaction conditions obtained for the fluorinated sample may in some cases differ from those of the non-fluorinated parent substrate. Furthermore, despite the enormous spectral width of  $^{19}\text{F}$  NMR spectra, substances with complex coupling patterns, or reactions with little change in the chemical environment around the fluorine probe may still exhibit significant signal overlap. Compounds that exhibit dynamic behavior over the time scale of the measurement, such as fluorinated cycloalkanes, may cause line-broadening, complicating quantification by  $^{19}\text{F}$  NMR. Finally, the relaxation agent may react with aggressive analytes, interfering with its ability to act as a  $T_1$  relaxation agent. Therefore, it is recommended that the yield measured in the presence of a relaxation agent is regularly compared to that obtained in the control experiment in the absence of the relaxation agent.

## Conclusions

This protocol facilitates rapid and reliable quantification of reactions using benchtop  $^{19}\text{F}$  qNMR spectroscopy. Its utility for reaction optimization is demonstrated for three representative model reactions, a Buchwald-Hartwig amination, a Suzuki coupling, and a C–H activation reaction. The protocol enables quantification of a wide variety of analytes in as little as 32 s using a paramagnetic non-

shifting relaxation agent. Reliable quantification is possible even for signals as much as 100 ppm away from the center frequency. In all cases, the results obtained with this rapid measurement protocol were within error of those obtained without a relaxation agent and elongated repetition times. Using this method, reaction analysis is no longer the bottleneck of reaction optimization. We are convinced that this protocol will find broad application in reaction discovery and optimization.

## References

---

1. Carlson, R. & Carlson, J. *Design and Optimization in Organic Synthesis, Volume 24 - 1st Edition*. vol. 24 (Elsevier, 1992).
2. Markert, C., Rösel, P. & Pfaltz, A. Combinatorial Ligand Development Based on Mass Spectrometric Screening and a Double Mass-Labeling Strategy. *J. Am. Chem. Soc.* **130**, 3234–3235 (2008).
3. McNally, A., Prier, C. K. & MacMillan, D. W. C. Discovery of an  $\alpha$ -Amino C–H Arylation Reaction Using the Strategy of Accelerated Serendipity. *Science* **334**, 1114–1117 (2011).
4. Robbins, D. W. & Hartwig, J. F. A Simple, Multidimensional Approach to High-Throughput Discovery of Catalytic Reactions. *Science* **333**, 1423–1427 (2011).
5. Hopkinson, M. N., Gómez-Suárez, A., Teders, M., Sahoo, B. & Glorius, F. Accelerated Discovery in Photocatalysis using a Mechanism-Based Screening Method. *Angew. Chem. Int. Ed.* **55**, 4361–4366 (2016).
6. Troshin, K. & Hartwig, J. F. Snap deconvolution: An informatics approach to high-throughput discovery of catalytic reactions. *Science* **357**, 175–181 (2017).
7. Collins, K. D. & Glorius, F. A robustness screen for the rapid assessment of chemical reactions. *Nat. Chem.* **5**, 597–601 (2013).
8. Prieto Kullmer, C. N. *et al.* Accelerating reaction generality and mechanistic insight through additive mapping. *Science* **376**, 532–539 (2022).
9. Pitzer, L., Schäfers, F. & Glorius, F. Rapid Assessment of the Reaction-Condition-Based Sensitivity of Chemical Transformations. *Angew. Chem. Int. Ed.* **58**, 8572–8576 (2019).
10. Schafer, W., Bu, X., Gong, X., Joyce, L. A. & Welch, C. J. High-Throughput Analysis for High-Throughput Experimentation in Organic Chemistry. in *Comprehensive Organic Synthesis (Second Edition)* (ed. Knochel, P.) 28–53 (Elsevier, 2014). doi:10.1016/B978-0-08-097742-3.00921-6.
11. Vries, J. G. de & Vries, A. H. M. de. The Power of High-Throughput Experimentation in Homogeneous Catalysis Research for Fine Chemicals. *Eur. J. Org. Chem.* **2003**, 799–811 (2003).
12. Krska, S. W., DiRocco, D. A., Dreher, S. D. & Shevlin, M. The Evolution of Chemical High-Throughput Experimentation To Address Challenging Problems in Pharmaceutical Synthesis. *Acc. Chem. Res.* **50**, 2976–2985 (2017).
13. Mennen, S. M. *et al.* The Evolution of High-Throughput Experimentation in Pharmaceutical Development and Perspectives on the Future. *Org. Process Res. Dev.* **23**, 1213–1242 (2019).
14. Isbrandt, E. S., Sullivan, R. J. & Newman, S. G. High Throughput Strategies for the Discovery and Optimization of Catalytic Reactions. *Angew. Chem. Int. Ed.* **58**, 7180–7191 (2019).
15. Buitrago Santanilla, A. *et al.* Nanomole-scale high-throughput chemistry for the synthesis of complex molecules. *Science* **347**, 49–53 (2015).
16. Welch, C. J. High throughput analysis enables high throughput experimentation in pharmaceutical process research. *React. Chem. Eng.* **4**, 1895–1911 (2019).
17. Welch, C. J. *et al.* MISER chromatography (multiple injections in a single experimental run): the chromatogram is the graph. *Tetrahedron Asymmetry* **21**, 1674–1681 (2010).
18. Holzgrabe, U. Quantitative NMR spectroscopy in pharmaceutical applications. *Prog. Nucl. Magn. Reson. Spectrosc.* **57**, 229–240 (2010).
19. Marquez, B. L. & Williamson, R. T. Quantitative Applications of Nmr Spectroscopy. in *Chemical Engineering in the Pharmaceutical Industry* 133–149 (John Wiley & Sons, Ltd, 2019). doi:10.1002/9781119600800.ch7.
20. Diehl, B., Holzgrabe, U., Monakhova, Y. & Schönberger, T. Quo Vadis qNMR? *J. Pharm. Biomed. Anal.* **177**, 112847 (2020).
21. Mitchell, J., Gladden, L. F., Chandrasekera, T. C. & Fordham, E. J. Low-field permanent magnets for industrial process and quality control. *Prog. Nucl. Magn. Reson. Spectrosc.* **76**, 1–60 (2014).
22. Danieli, E., Perlo, J., Blümich, B. & Casanova, F. Small Magnets for Portable NMR Spectrometers. *Angew. Chem. Int. Ed.* **49**, 4133–4135 (2010).
23. Dalitz, F., Cudaj, M., Maiwald, M. & Guthausen, G. Process and reaction monitoring by low-field NMR spectroscopy. *Prog. Nucl. Magn. Reson. Spectrosc.* **60**, 52–70 (2012).
24. Dyga, M., Oppel, C. & Gooßen, L. J. RotoMate: An open-source, 3D printed autosampler for use with benchtop nuclear magnetic resonance spectrometers. *HardwareX* **10**, e00211 (2021).
25. Matheis, C., Jouvin, K. & Goossen, L. J. Sandmeyer Difluoromethylation of (Hetero-)Arenediazonium Salts. *Org. Lett.* **16**, 5984–5987 (2014).

26. Danoun, G. *et al.* Sandmeyer Trifluoromethylation. *Synthesis* **46**, 2283–2286 (2014).
27. Bertoli, G., Exner, B., Evers, M. V., Tschulik, K. & Gooßen, L. J. Metal-free trifluoromethylthiolation of arenediazonium salts with Me<sub>4</sub>N<sup>+</sup>SCF<sub>3</sub><sup>-</sup>. *J. Fluor. Chem.* **210**, 132–136 (2018).
28. Ou, Y. & Gooßen, L. J. Copper-Mediated Synthesis of (Diethylphosphono)difluoromethyl Thioethers from Diazonium Salts, NaSCN, and TMS-CF<sub>2</sub>PO(OEt)<sub>2</sub>. *Asian J. Org. Chem.* **8**, 650–653 (2019).
29. Weber, P. *et al.* A Highly Active Ylide-Functionalized Phosphine for Palladium-Catalyzed Aminations of Aryl Chlorides. *Angew. Chem. Int. Ed.* **58**, 3203–3207 (2019).
30. Sivendran, N. *et al.* Photochemical Sandmeyer-type Halogenation of Arenediazonium Salts. *Chem. Eur. J.* **28**, e202103669 (2022).
31. Bertoli, G. *et al.* C-H Fluoromethoxylation of Arenes by Photoredox Catalysis. *Angew. Chem. Int. Ed.* **62**, e202215920 (2023).
32. Holzgrabe, U. Quantitative NMR Spectroscopy in Pharmaceutical R&D. in *eMagRes* 45–56 (John Wiley & Sons, Ltd, 2015). doi:10.1002/9780470034590.emrstm1399.
33. Schoenberger, T. ENFSI Guideline for qNMR Analysis. [https://enfsi.eu/wp-content/uploads/2017/06/qNMR-Guideline\\_version001.pdf](https://enfsi.eu/wp-content/uploads/2017/06/qNMR-Guideline_version001.pdf) (2019).
34. Dolbier, W. R. Jr. *Guide to Fluorine NMR for Organic Chemists*. (John Wiley & Sons, Ltd, 2016). doi:10.1002/9781118831106.
35. Howe, P. W. A. Recent developments in the use of fluorine NMR in synthesis and characterisation. *Prog. Nucl. Magn. Reson. Spectrosc.* **118–119**, 1–9 (2020).
36. O'Hagan, D. Understanding organofluorine chemistry. An introduction to the C–F bond. *Chem. Soc. Rev.* **37**, 308–319 (2008).
37. Purser, S., Moore, P. R., Swallow, S. & Gouverneur, V. Fluorine in medicinal chemistry. *Chem. Soc. Rev.* **37**, 320–330 (2008).
38. Inoue, M., Sumii, Y. & Shibata, N. Contribution of Organofluorine Compounds to Pharmaceuticals. *ACS Omega* **5**, 10633–10640 (2020).
39. Campbell, M. G. & Ritter, T. Modern Carbon–Fluorine Bond Forming Reactions for Aryl Fluoride Synthesis. *Chem. Rev.* **115**, 612–633 (2015).
40. Champagne, P. A., Desroches, J., Hamel, J.-D., Vandamme, M. & Paquin, J.-F. Monofluorination of Organic Compounds: 10 Years of Innovation. *Chem. Rev.* **115**, 9073–9174 (2015).
41. Landelle, G., Bergeron, M., Turcotte-Savard, M.-O. & Paquin, J.-F. Synthetic approaches to monofluoroalkenes. *Chem. Soc. Rev.* **40**, 2867–2908 (2011).
42. Umemoto, T. *et al.* Power- and structure-variable fluorinating agents. The N-fluoropyridinium salt system. *J. Am. Chem. Soc.* **112**, 8563–8575 (1990).
43. Watson, D. A. *et al.* Formation of ArF from LPdAr(F): Catalytic Conversion of Aryl Triflates to Aryl Fluorides. *Science* **325**, 1661–1664 (2009).
44. Fier, P. S. & Hartwig, J. F. Selective C-H Fluorination of Pyridines and Diazines Inspired by a Classic Amination Reaction. *Science* **342**, 956–960 (2013).
45. Molnár, I. G. & Gilmour, R. Catalytic Difluorination of Olefins. *J. Am. Chem. Soc.* **138**, 5004–5007 (2016).
46. Prakash, G. K. S. & Yudin, A. K. Perfluoroalkylation with Organosilicon Reagents. *Chem. Rev.* **97**, 757–786 (1997).
47. Tomashenko, O. A. & Grushin, V. V. Aromatic Trifluoromethylation with Metal Complexes. *Chem. Rev.* **111**, 4475–4521 (2011).
48. Cho, E. J. *et al.* The Palladium-Catalyzed Trifluoromethylation of Aryl Chlorides. *Science* **328**, 1679–1681 (2010).
49. Charpentier, J., Früh, N. & Togni, A. Electrophilic Trifluoromethylation by Use of Hypervalent Iodine Reagents. *Chem. Rev.* **115**, 650–682 (2015).
50. Umemoto, T. & Ishihara, S. Power-variable electrophilic trifluoromethylating agents. S-, Se-, and Te-(trifluoromethyl)dibenzothio-, -seleno-, and -tellurophenium salt system. *J. Am. Chem. Soc.* **115**, 2156–2164 (1993).
51. Hafner, A. & Bräse, S. Ortho-Trifluoromethylation of Functionalized Aromatic Triazines. *Angew. Chem. Int. Ed.* **51**, 3713–3715 (2012).
52. Le, C., Chen, T. Q., Liang, T., Zhang, P. & MacMillan, D. W. C. A radical approach to the copper oxidative addition problem: Trifluoromethylation of bromoarenes. *Science* **360**, 1010–1014 (2018).
53. Britton, R. *et al.* Contemporary synthetic strategies in organofluorine chemistry. *Nat. Rev. Methods Primer* **1**, 1–22 (2021).
54. Wiesenfeldt, M. P., Nairoukh, Z., Li, W. & Glorius, F. Hydrogenation of fluoroarenes: Direct access to all-*cis*-(multi)fluorinated cycloalkanes. *Science* **357**, 908–912 (2017).
55. Chen, K., Berg, N., Gschwind, R. & König, B. Selective Single C(sp<sup>3</sup>)–F Bond Cleavage in Trifluoromethylarenes: Merging Visible-Light Catalysis with Lewis Acid Activation. *J. Am. Chem. Soc.* **139**, 18444–18447 (2017).

56. Dolbier, W. R. Fluorine chemistry at the millennium. *J. Fluor. Chem.* **126**, 157–163 (2005).
57. Rosenau, C. P., Jelier, B. J., Gossert, A. D. & Togni, A. Exposing the Origins of Irreproducibility in Fluorine NMR Spectroscopy. *Angew. Chem. Int. Ed.* **57**, 9528–9533 (2018).
58. Power, J. E. *et al.* Increasing the quantitative bandwidth of NMR measurements. *Chem. Commun.* **52**, 2916–2919 (2016).
59. Yamazaki, T., Saito, T. & Ihara, T. A new approach for accurate quantitative determination using fluorine nuclear magnetic resonance spectroscopy. *J. Chem. Metrol.* **11**, 16–22 (2017).
60. Mattes, A. O. *et al.* Application of <sup>19</sup>F quantitative NMR to pharmaceutical analysis. *Concepts Magn. Reson. Part A* **45A**, e21422 (2016).
61. Excitation profile | Leuven NMR Core. [https://nmrcore.chem.kuleuven.be/knowledgebase/excitation\\_profile.php](https://nmrcore.chem.kuleuven.be/knowledgebase/excitation_profile.php).
62. Ellis, D. A., Martin, J. W., Muir, D. C. G. & Mabury, S. A. Development of an <sup>19</sup>F NMR Method for the Analysis of Fluorinated Acids in Environmental Water Samples. *Anal. Chem.* **72**, 726–731 (2000).
63. Schoenberger, T., Monakhova, Y. B., Lachenmeier, D. W. & Kuballa, T. Guide to NMR method development and validation - Part I - Identification and quantification.pdf. [https://eurolab-d.de/files/guide\\_to\\_nmr\\_method\\_development\\_and\\_validation\\_-\\_part\\_i\\_identification\\_and\\_quantification\\_may\\_2014.pdf](https://eurolab-d.de/files/guide_to_nmr_method_development_and_validation_-_part_i_identification_and_quantification_may_2014.pdf) (2014).
64. Bloembergen, N., Purcell, E. M. & Pound, R. V. Relaxation Effects in Nuclear Magnetic Resonance Absorption. *Phys. Rev.* **73**, 679–712 (1948).
65. Callaghan, P. T. *Principles of Nuclear Magnetic Resonance Microscopy*. (Clarendon Press, 1993).
66. Claridge, T. D. W. Chapter 2 - Introducing High-Resolution NMR. in *High-Resolution NMR Techniques in Organic Chemistry (Third Edition)* (ed. Claridge, T. D. W.) 11–59 (Elsevier, 2016). doi:10.1016/B978-0-08-099986-9.00002-6.
67. Levy, G. C. & Komoroski, R. A. Paramagnetic relaxation reagents. Alternatives or complements to lanthanide shift reagents in nuclear magnetic resonance spectral analysis. *J. Am. Chem. Soc.* **96**, 678–681 (1974).
68. Kocman, V., Di Mauro, G. M., Veglia, G. & Ramamoorthy, A. Use of paramagnetic systems to speed-up NMR data acquisition and for structural and dynamic studies. *Solid State Nucl. Magn. Reson.* **102**, 36–46 (2019).
69. Mortimer, R. D. & Dawson, B. A. Using fluorine-19 NMR for trace analysis of fluorinated pesticides in food products. *J. Agric. Food Chem.* **39**, 1781–1785 (1991).
70. MestreNova Manual. [https://mnova.pl/files/download/MestReNova-12-0-0\\_Manual.pdf](https://mnova.pl/files/download/MestReNova-12-0-0_Manual.pdf) (2017).
71. Guide to NMR Method Development and Validation – Part 1: Identification and Quantification. in *Handbook of Transnational Economic Governance Regimes* 1041–1053 (Brill | Nijhoff, 2010). doi:10.1163/ej.9789004163300.i-1081.897.
72. Hartwig, J. F. Evolution of a Fourth Generation Catalyst for the Amination and Thioetherification of Aryl Halides. *Acc. Chem. Res.* **41**, 1534–1544 (2008).
73. Ruiz-Castillo, P. & Buchwald, S. L. Applications of Palladium-Catalyzed C–N Cross-Coupling Reactions. *Chem. Rev.* **116**, 12564–12649 (2016).
74. Biafora, A., Krause, T., Hackenberger, D., Belitz, F. & Gooßen, L. J. ortho-C–H Arylation of Benzoic Acids with Aryl Bromides and Chlorides Catalyzed by Ruthenium. *Angew. Chem.* **128**, 14972–14975 (2016).

## Acknowledgements

---

Funded by the Deutsche Forschungsgemeinschaft (DFG, German Research Foundation) under Germany's Excellence Strategy – EXC 2033 – 390677874 – RESOLV and SFBTRR88 “3MET”, BMBF, the state of NRW (Center of Solvation Science “ZEMOS”), and the Fonds der Chemischen Industrie (FCI, Liebig Fellowship for M.P.W.). We thank Martin Gartmann for assistance with NMR expertise and proofreading. We thank Umicore AG & Co. KG for the donation of catalysts and Dr. K. Gooßen for proofreading.

## Competing interests

---

The authors declare no competing interests.

## Additional Information

---

Supplementary Information is available for this paper.

All relevant data are available in the manuscript or in the accompanying supporting information.

Correspondence and requests for materials should be addressed to Mario Wiesenfeldt.